Annual and Semiannual variation in the ionospheric F2-layer Electron density over the Indian zone and effect of solar activity on it

ABSTRACT

In situ measurement carried out by the Retarding potential Analyzer (RPA) on board SROSS C2 and ROCSAT during 1995 to 2003 covering ascending and descending periods of solar cycle 23 over Indian equatorial and low latitude were used to study the annual and semiannual variation of electron density at the topside F region. The 'Semiannual anomaly' which represent the electron density in equinox (March, April, September and October) is greater than that at solstice (May, June, July, August, November, December, January and February). The 'annual anomaly' which represents the electron density in winter (November, December, January, February) is higher than that in summer (May, June, July, August). The analysis has been carried out for the geomagnetic equator and $\pm 10^{o}$ magnetic latitudes. Observations reveal the existence of an equatorial asymmetry during daytime (10:00 – 14:00 hrs.) with higher electron density in spring (March, April) than in autumn (September, October) for both ascending and descending leg of the solar cycle. At the peak of the solar cycle, the density becomes equal for both equinoxes. Nighttime (22:00 – 00:00 hrs.) density in autumn is higher than that in spring for the ascending half of the solar cycle, becomes equal for both the equinoxes around the peak of the solar cycle. In the descending half the vernal density becomes higher than the autumnal density. The periodograms obtained from a Fourier analysis of the daytime average density shows that the annual variation is dominant over the semiannual variations for low to moderate solar activity whereas the semiannual peak becomes dominant over annual peak for high solar activity irrespective of the latitudes. At night, however, latitudinal differences have been observed. The annual variation is stronger than the semiannual variation at 10^{o} N for low to moderate solar activity while for high solar activity the situation reverses. At 10^{o} S and the magnetic equator, the annual variation is dominant for all levels of solar activity. Amplitude of the annual variation is higher in winter compared to that in summer. The physical and dynamical processes responsible for the observed annual and semi-annual trends in topside density will be identified and discussed.

Keywords: Electron density, F-region, equatorial ionosphere, annual and semiannual variation.

1. INTRODUCTION

In the equatorial region earth's magnetic field lines are perfectly horizontal within a narrow belt of about $\pm 3^{o}$ geomagnetic latitude gives rise to the electrojet current between

altitudes of 70 km and 140 km and it is transferred almost undiminished to higher altitudes, to affect deeply the entire low latitude region. The electrojet current gives rise to the equatorial ionization anomaly (EIA), the fountain effect; the post sunset equatorial anomaly (PEA), noon bite-out, spread F etc. Because of the physical structure of the equatorial region the equatorial ionosphere has been studied theoretically and experimentally since long (Moffett ,1979; Anderson, 1981; Walker et al., 1994; bailey and Balan, 1996; Rishbeth, 2000 and references therein). In India also equatorial ionosphere has been studied extensively. The Indian satellite SROSS C2 provides data from December 1994 to July 2001 over the equatorial zone. Using SROSS C2 data the variability of F region ionosphere has been studied (Bhuyan et al., 2002 a, b; Bhuyan et al., 2003; Bhuyan et al. (2006); Niranjan et al., 2003). Bhuyan et al. (2006) have reported the effect of solar activity on local time and seasonal variations of electron temperature measured by the SROSS C2 during the low to moderate solar activity period from 1995 to 1998 over the Indian subcontinent. They have found positive correlation of both daytime (10:00-14:00 hr) and night-time (02:00-22:00 hr) electron temperature with solar activity. Besides diurnal, seasonal latitudinal and solar cycle variation ionospheric parameters also exhibit annual and semi-annual variation. The 'Semiannual anomaly' which represent the electron density in equinox (March, April, September and October) is greater than that at solstice (May, June, July, August, November, December, January and February). The 'annual anomaly' which represents the electron density in winter (November, December, January, February) is higher than that in summer (May, June, July, August).

Ionospheric parameters such as peak electron density of the ionospheric F2 layer (NmF2), the height of the F2-layer peak (hmF2), electron density, total electron content, electron temperature exhibits annual and semiannual variations. Rishbeth et al. 1999, used ionosonde data from sixteen stations to make an extensive study on annual and semiannual variations in hmF2 over mid latitudes. Zou et al. 2000 used ionosonde data to study annual, seasonal and semiannual variations of NmF2 and hmF2 over Slough (52^{o} N, 1^{o} W), Kerguelen (49^{o} S, 70^{o} E), Wallops Island (38^{o} N, 75^{o} W), Hobart (43^{o} S, 147^{o} E), Wakkanai (38^{o} N, 142^{o} E), Port Stanley (52^{o} S, 58^{o} W) and compared with the coupled thermosphere-ionosphere-plasmasphere computational model (CTIP) for geomagnetically quiet conditions.

Su et al. 1998 observed annual and seasonal variations in the low-latitude topside electron density using observations made by the Hinotori satellite and the Sheffield University Plasmasphere Ionosphere Model (SUPIM). Zhao et al. 2008 used the NASA – JPL global ionospheric maps of total electron content (TEC), to construct TEC maps (TEC vs. magnetic local time MLT, and magnetic latitude MLAT) in the interval from 1999 to 2005. Using these TEC maps, they investigated in detail the TEC climatology with an emphasis on the quantitative presentation for local time and latitudinal changes in the seasonal, annual and semiannual anomalies of the ionospheric TEC. Yufei et al. 2010 used observations of Langmuir Probe Instrument (ISL, Instrument Sonde de Langmuir) onboard the DEMETER satellite during four years from 2006 to 2009 to analyze the annual and semiannual variation of electron density (Ne) and electron temperature (Te) at 660 km altitude covering an area with 10^{o} in longitude and 2^{o} in latitude. Zheng et al. 2016 studied diurnal, seasonal, annual and semiannual variation of critical frequency of the F2 layer (f_oF2), the peak height of the F2 layer (h_mF2) and the scale height at h_mF2 (H_T) from 2006 to 2012 (ascending phase of solar activity) at Haninan (19.5^{o} N, 109.1^{o}E, MLat 9.7^{o}N), Irkutrk (52.4^{o}N,104.3^{o}E, MLat. 42.5^{o} N), and Norilsk (69.2^{o} N, 88.0^{o}E, MLat 59.8^{o} N) stations. They used manual scaled digisonde ionogram data and compared with data obtained by a satellite occultation and TEC map.

In this paper we present the yearly variation of electron density at 500 km/600 km altitudes The electron density measured by the SROSS C2 satellite during the period January 1995 to July 2001 has been studied over three latitudes $\pm10^{o}$ of the geomagnetic equator and over the geomagnetic equator. The data are grouped into bins of $\pm2.5^{o}$ in latitude and 1 hour in local time. over $\pm10^{o}$ magnetic and the magnetic equator of the Indian subcontinent for the solar cycle 23. The time mentioned in the paper is local time for India. Local time indicates the time of a place determined on the basis of the apparent movement of the sun. Universal time (UT) is a time standard based on Earth's rotation.

1.1 DATA COLLECTION DISSEMINATION AND ANALYSIS

The RPA payload on board SROSS C2 satellite did not have any on board memory for data storage unlike those on other satellites like Hinotori. Hence the payload is switched on during

the satellite visibilities over that particular ground station and data was collected at that T/M tracking station. As a result, the latitude/longitude coverage of data gets restricted to limited region. Data could be collected at ISRO's Bangalore (12.5^{o} N, 77.3^{o} E) and Lucknow (26.8^{o} N, 80.8^{o} E) ground stations. Data could also be collected from the foreign ground station located in Mauritius (20^{o} S, 56^{o} E). But due to some operational problems regular data collection was under taken from the Bangalore ground station only. During campaign mode data was collected from Lucknow and sometimes from Mauritius ground station also, which gave an extended visibility of the satellite. The SROSS C2 satellite had orbital period of 90 minutes, making approximately 16 orbits in 24 hours, out of which two high elevation passes in daytime conditions and two during night were visible from a single telemetry station. Data was collected from one daytime pass and one night-time pass for RPA on a regular basis. Depending on the satellite elevation angles as viewed from the ground station, satellite visibility varies from 7 to 12 minutes. During a high elevation pass data coverage could be from 5^{o} S to 30^{o} N and with an extended visibility from Lucknow ground station data coverage could be from 5^{o} S up to 38^{o} N. In terms of longitudinal coverage data coverage could be from 50^{o} E to around 100^{o} E. In a low elevation pass latitude coverage might be as low as 10^{o} S. The RPA data were collected only in those orbits, which had sufficiently high elevation from the tracking stations for having larger data coverage.

Basic measurement in both electron and ion RPA consisted of collector current against retarding grid voltage (I – V characteristic curve). A least square fitting technique has been used to derive electron temperature from the slope of the linear region of the I – V characteristic curve. The ion RPA is used to derive a composite I – V curve for ions O+, O2+, NO+, H+, He+ and ion density Ni (ne) obtained from the I – V curve by fitting a non-linear curve to the observed characteristic by method of iteration. Garg and Das 1995 had discussed some aspects of the aeronomy experiment on SROSS C2. In addition to this measured data there were other data generated in the payload for each measurement. This data was in the form of partly in analog and the rest in the digital form. Each RPA measurement was carried out in time duration of 22 msec. This data was arranged in 9 words of 16 bits each, called RPA telemetry format. After the recording of Telemetry data, off line processing of satellite data was done at ISRO Satellite Tracking Centre (ISTRAC), Bangalore to generate attitude and orbital parameters of the

satellite, separation of payload data from rest of the data and house keeping parameters. Off line processing of data recorded at Lucknow and Mauritius was also done at Bangalore station only.

2. Results and Analysis

For this analysis we have used the electron density Ne data as measured by the Retarding Potential analyzer (RPA) on board SROSS C2 and ROCSAT-1 for the period 1995-2000 and 2001-2003 respectively. Fig. 1 shows the month-to-month variation of daytime (10.00 – 14:00 hrs.) electron density over 10 deg N, 0 deg mag. and 10 deg S latitudes. Daytime (10:00 – 14:00 hrs.) data for each month has been averaged. March, April (spring) and September, October (autumn) are considered as equinox months. Observations reveal the existence of an equinoctial asymmetry during daytime (10:00-14:00 hrs.) with higher electron density in spring than in autumn for both ascending and over descending leg of the solar cycle. The difference between the electron densities during daytime in equinoxes (spring and autumn) and summer months has been deduced and hence the percentage of increase has been calculated. The percentage increase of Ne in equinoxes over that in summer are given in Table I. The percentages have been derived after solar activity normalization

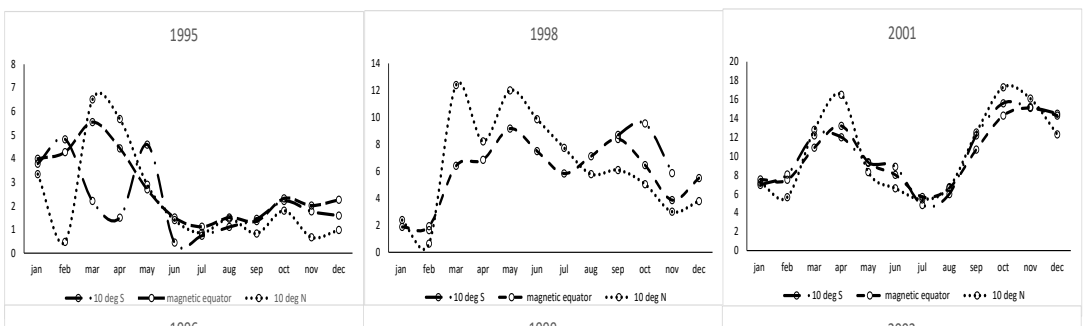

of observed electron density for each year. As shown in Table I the percentage increase of Ne in spring is higher than that in autumn over all the three latitudes. The rate of increase of Ne in spring slows with increasing solar activity. Further the difference between the levels of electron density in the two equinoxes decreases with increasing solar activity (Bakhram Nurtaev B. 2018) irrespective of latitude. Here F10.7 cm solar flux index with monthly averaged is used.

At night (22:00-00:00 hrs.), electron density is higher in autumn than that in Spring during low solar activity whereas for moderate and high solar activity electron density becomes higher in spring than in autumn in all the three latitudes (Fig. 2). The percentage increase of electron density in the equinoxes over that in summer are shown in Table II.

2.1 Fourier analysis

Fig. 3 – 8 shows periodograms obtained from Fourier analysis for the ± 10^{o} magnetic equator and over the magnetic equator from 1995 to 2003 and for both daytime and nighttime. The periodograms are obtained using the software, MATLAB. The periodograms show that during daytime the annual variation is dominant over the semiannual variation for the ascending half of the solar cycle while for the descending leg semiannual peak becomes stronger than the annual peak over all the three latitudes. Fig. 6 shows that over 10^{o} N magnetic latitude nighttime annual variation is dominant for the ascending leg and semiannual variation is dominant for the descending leg of the solar cycle. But over the magnetic equator and over 10^{o} S magnetic, the annual peak is dominant over the semiannual peak for all levels of solar activity. Due to unavailability of data some years are missing over 10^{o} S of the magnetic equator.

Table I: Percentage of increase of daytime electron density in equinoxes over the values in summer

Year	10o S magnetic		0o magnetic		10o N magnetic	
	spring	autumn	spring	autumn	spring	autumn
1995	94	34	83	5	137	-42
1996	121	43	100	4	178	-62
1997	80	29	73	5	117	-31
1998	35	14	33	7	51	2
1999	25	10	22	8	36	10
2000	21	9	17	8	29	13
2001	20	9	16	8	29	13
2002	21	9	17	8	30	13
2003	31	12	28	7	45	5

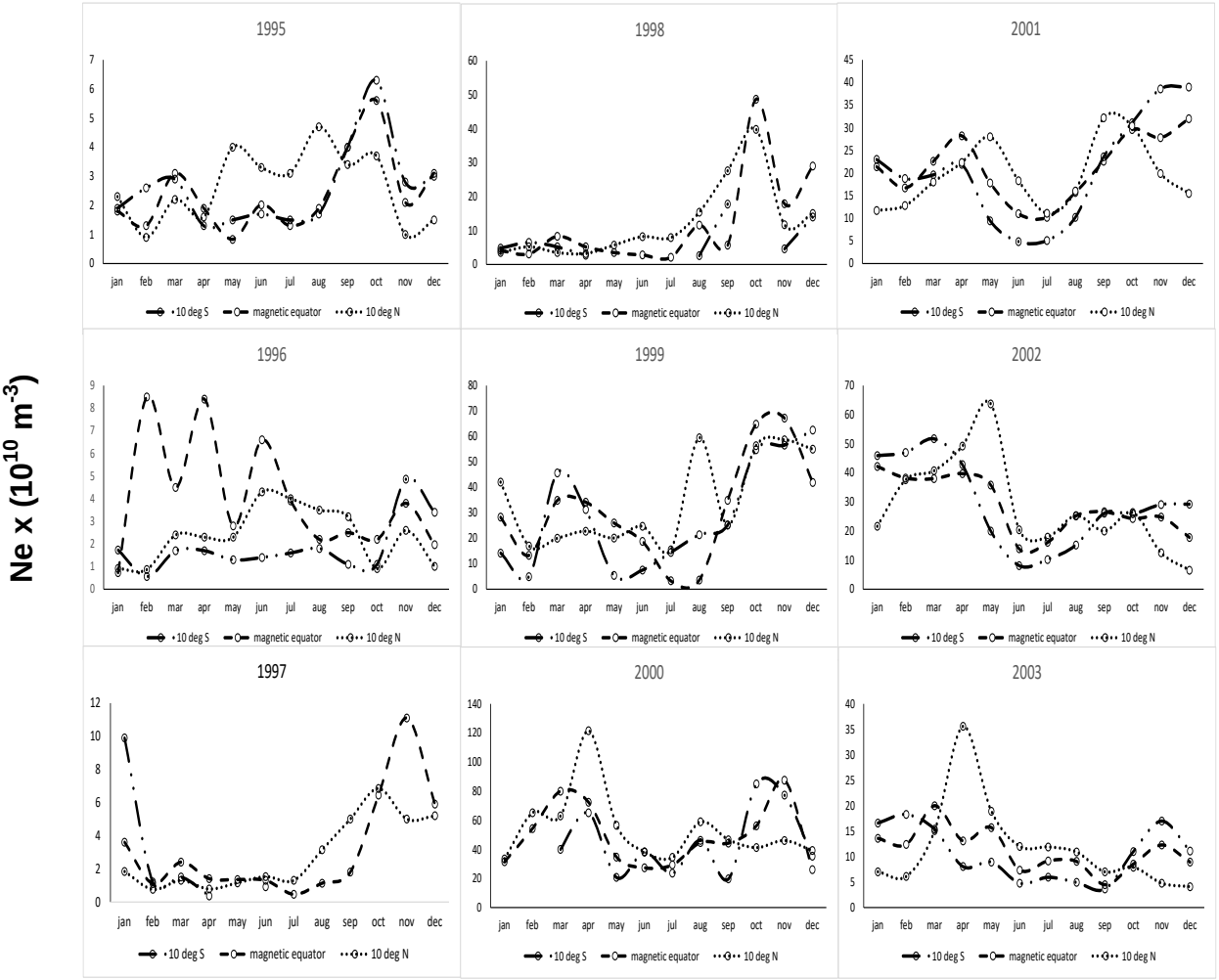

Yearly variation of electron density during nighttime at 500 km altitude.

Table II: Percentage of increase of nighttime electron density in equinoxes over the values in summer

Year	10^o S magnetic		0^o magnetic		10^o N magnetic	
	spring	autumn	spring	autumn	spring	autumn
1995	12	173	16	59	5	76
1996	-31	239	-46	97	-40	160
1997	30	146	32	49	16	56
1998	75	78	58	33	34	24
1999	83	65	61	31	36	20
2000	87	60	63	30	37	18
2001	87	60	63	30	37	18
2002	86	61	63	30	37	18
2003	79	72	59	32	25	22

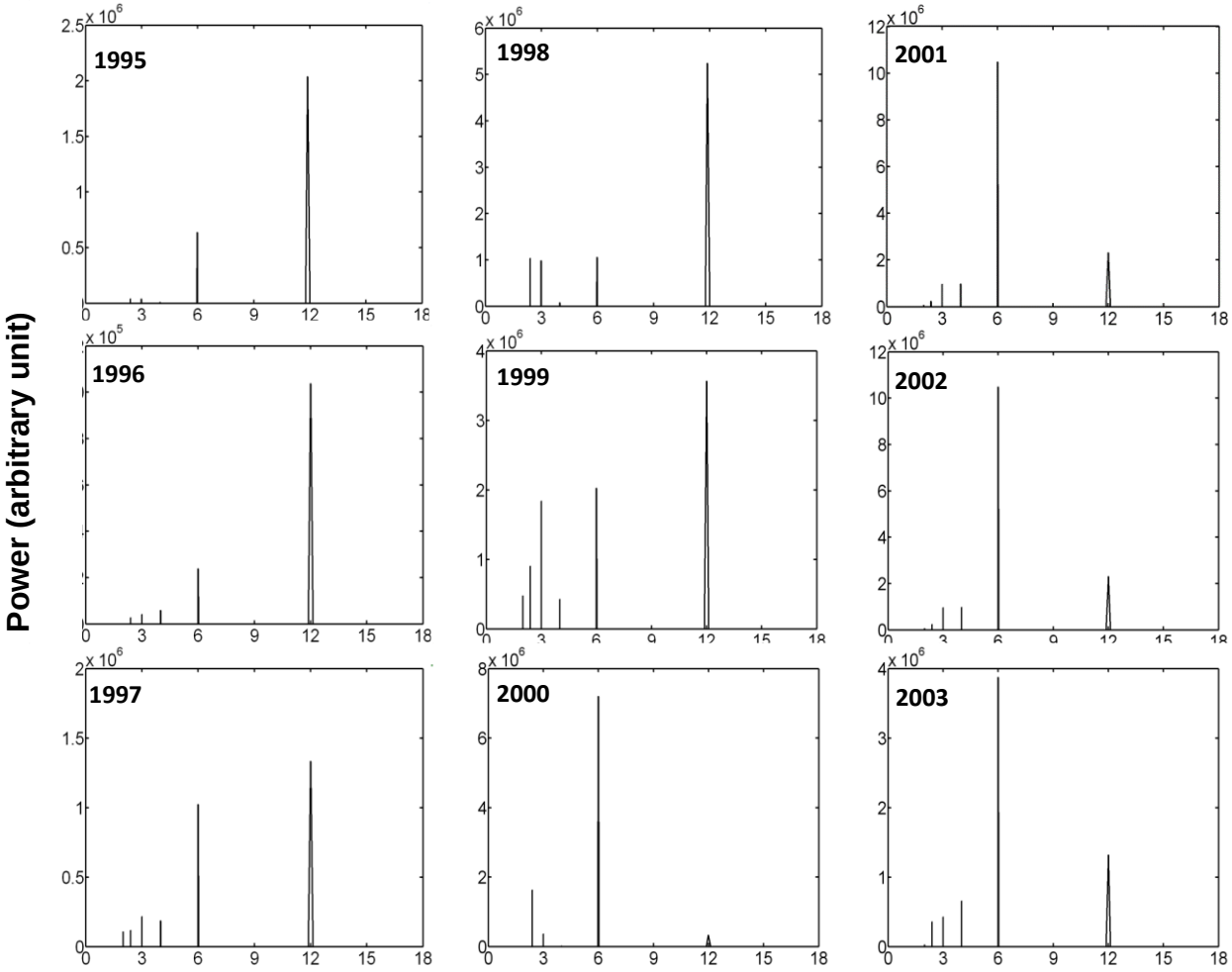

Periodogram of electron density during daytime over 10^{o} N magnetic.

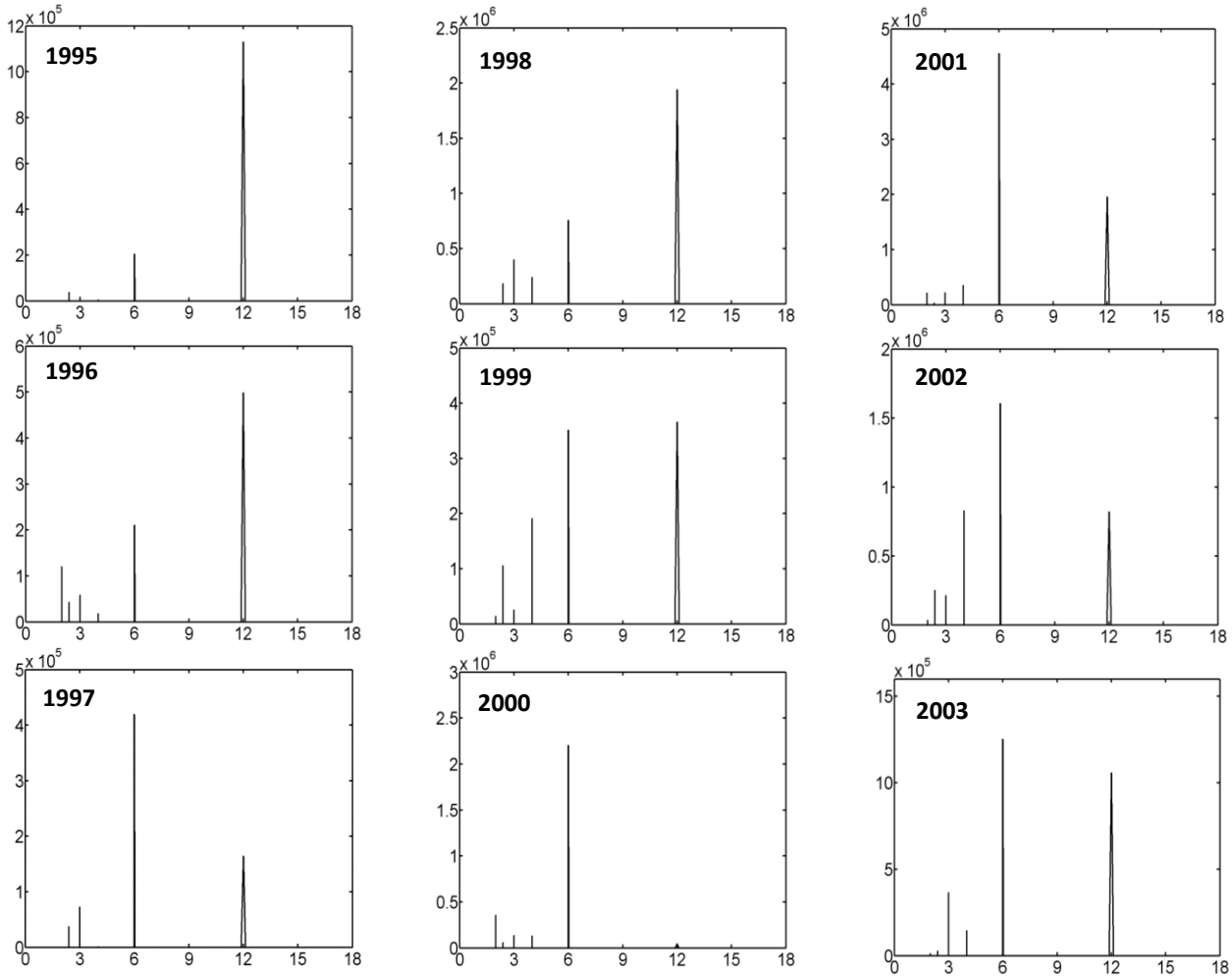

Periodogram of electron density during daytime over 0^{o} magnetic.

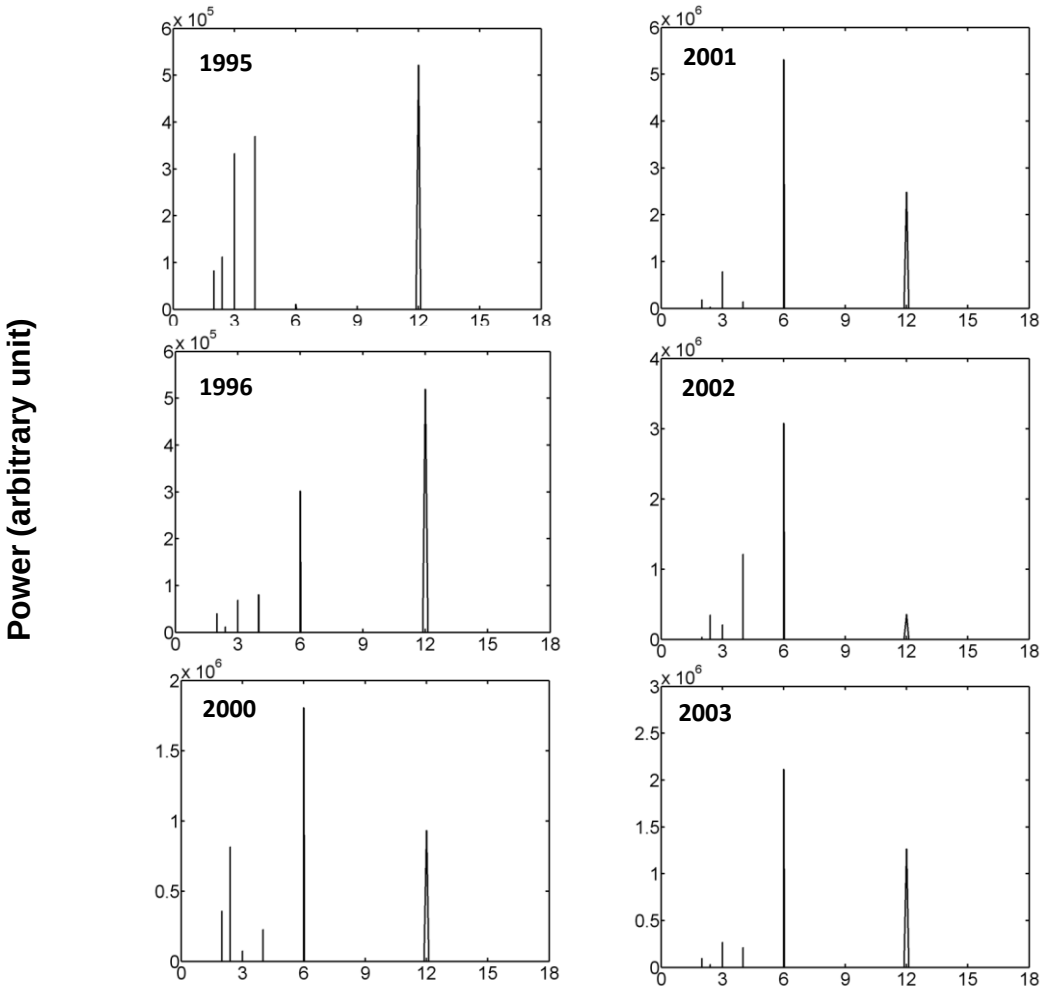

Periodogram of electron density during daytime over 10° S magnetic

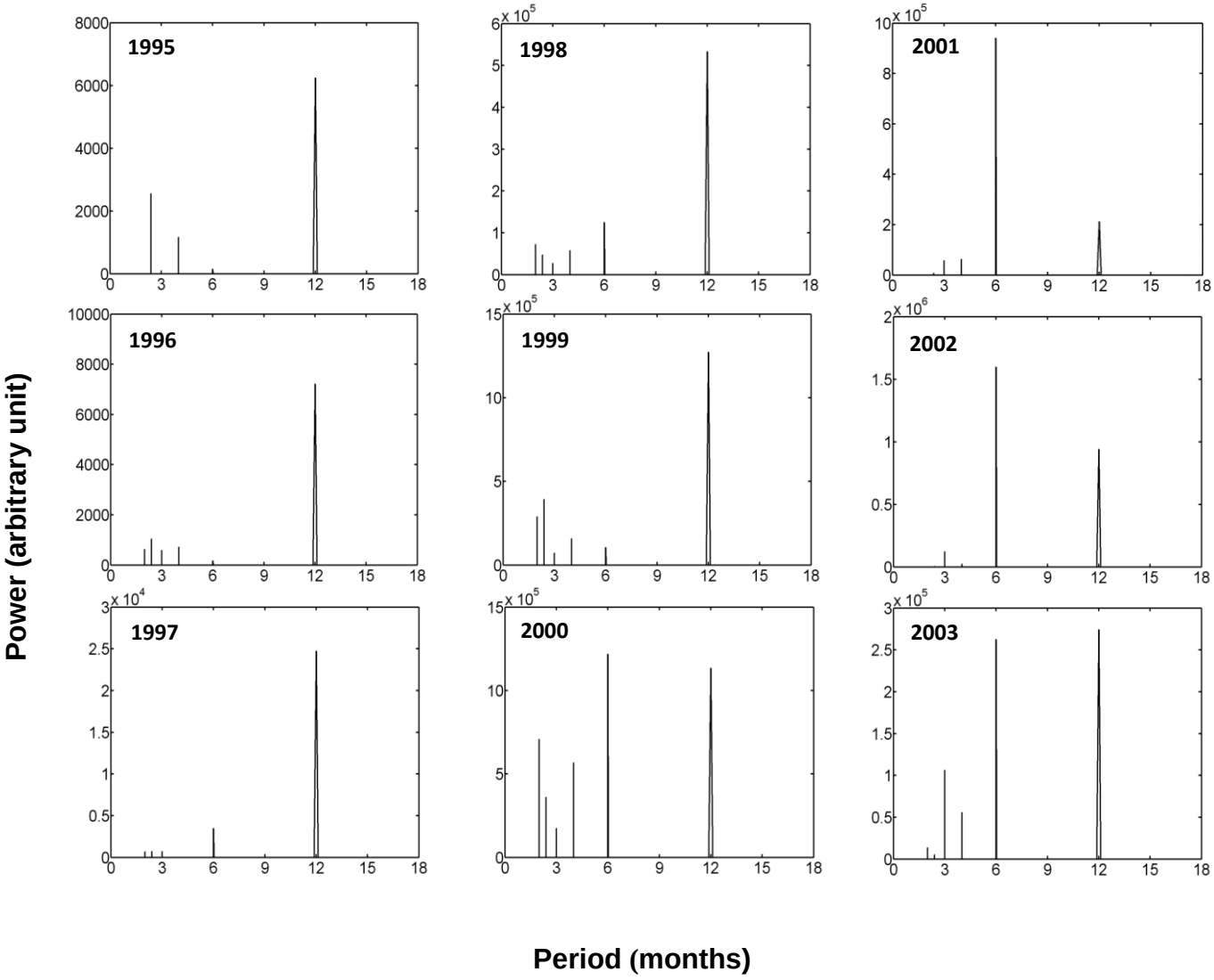

Periodogram of electron density during nighttime over 10° N magnetic.

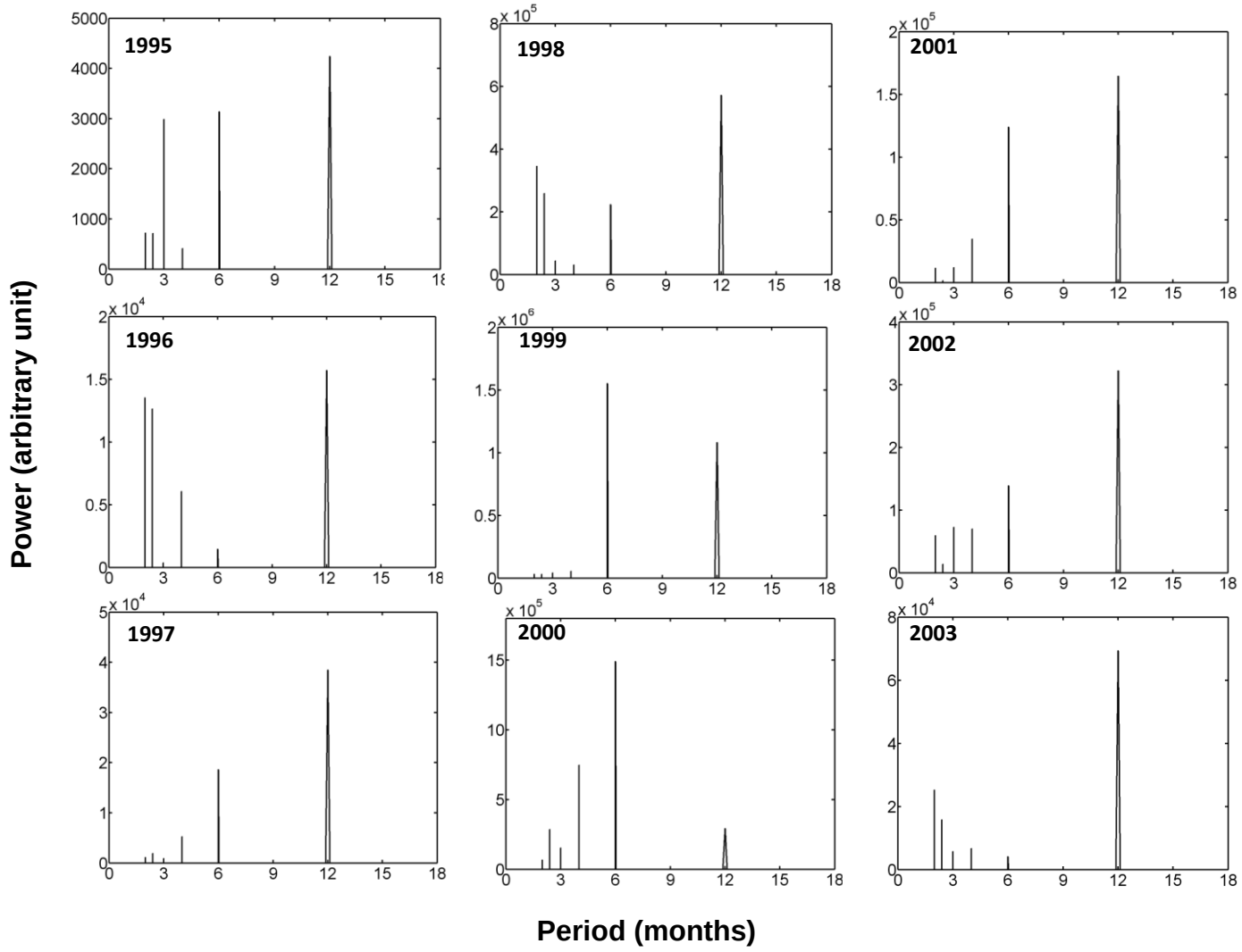

Periodogram of electron density during nighttime over 0° magnetic.

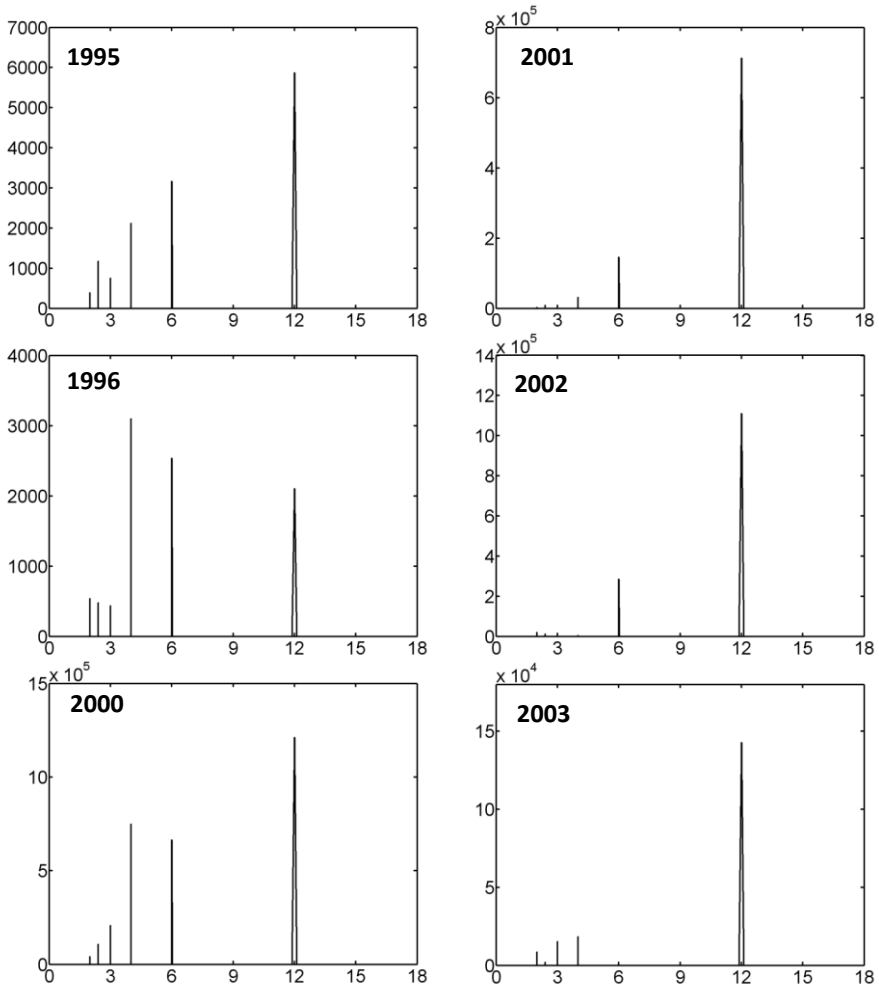

Periodogram of electron density during nighttime over 10° S magnetic.

2.1.1 Annual and semiannual components

Fig. 9 shows amplitudes of the mean (a_o), annual (a_1) and semiannual (a_2) components of Ne obtained from Fourier analysis plotted against the annual mean values of F10.7 over the three latitudes for daytime. A regression analysis indicates very good correlation of the annual means (~0.96 - ~0.98) and semiannual (~0.81- ~0.91) amplitudes with F10.7 cm solar flux. The annual component has poor correlation with F10.7 over all the three latitudes. Fig. 10 shows variation of nighttime amplitude a_o, a_1 and a_2 of Ne over $\pm 10^o$ magnetic and over the magnetic equator. The semiannual amplitude has better correlation with F10.7 over 10^o N magnetic than over the magnetic equator and over 10^o S of the magnetic equator. The nighttime annual amplitude has good correlation (~0.59 - ~0.92) with F10.7 over all the three latitudes.

As for phases, taking 1st January as 0 phase Tables III- V shows that while the annual phase fluctuates between summer and winter for both daytime and nighttime over all the three latitudes the semiannual variation is consistently near equinoxes irrespective of year and latitude.

2.3 Semiannual variation and MSIS model

The global distribution of daytime electron density at the F2 layer is essentially determined by the sun, and by the chemical composition of the neutral air upon which the sun's radiation acts. The important chemical parameter is the atomic/molecular ratios in the F2 layer, conveniently specified by the O/N_2 concentration ratio.

To determine the O/N_2 ratio at 500 km altitude we ran the Mass Spectrometer and Incoherent Scatter radar-2000 (MSIS-2000) model (J. M. Picone et al. 2002) for the $\pm 10^o$ magnetic and over the geomagnetic equator for each month of the corresponding years at the local time 12:00 LT and for A_p = 15 to represent average condition and for annual

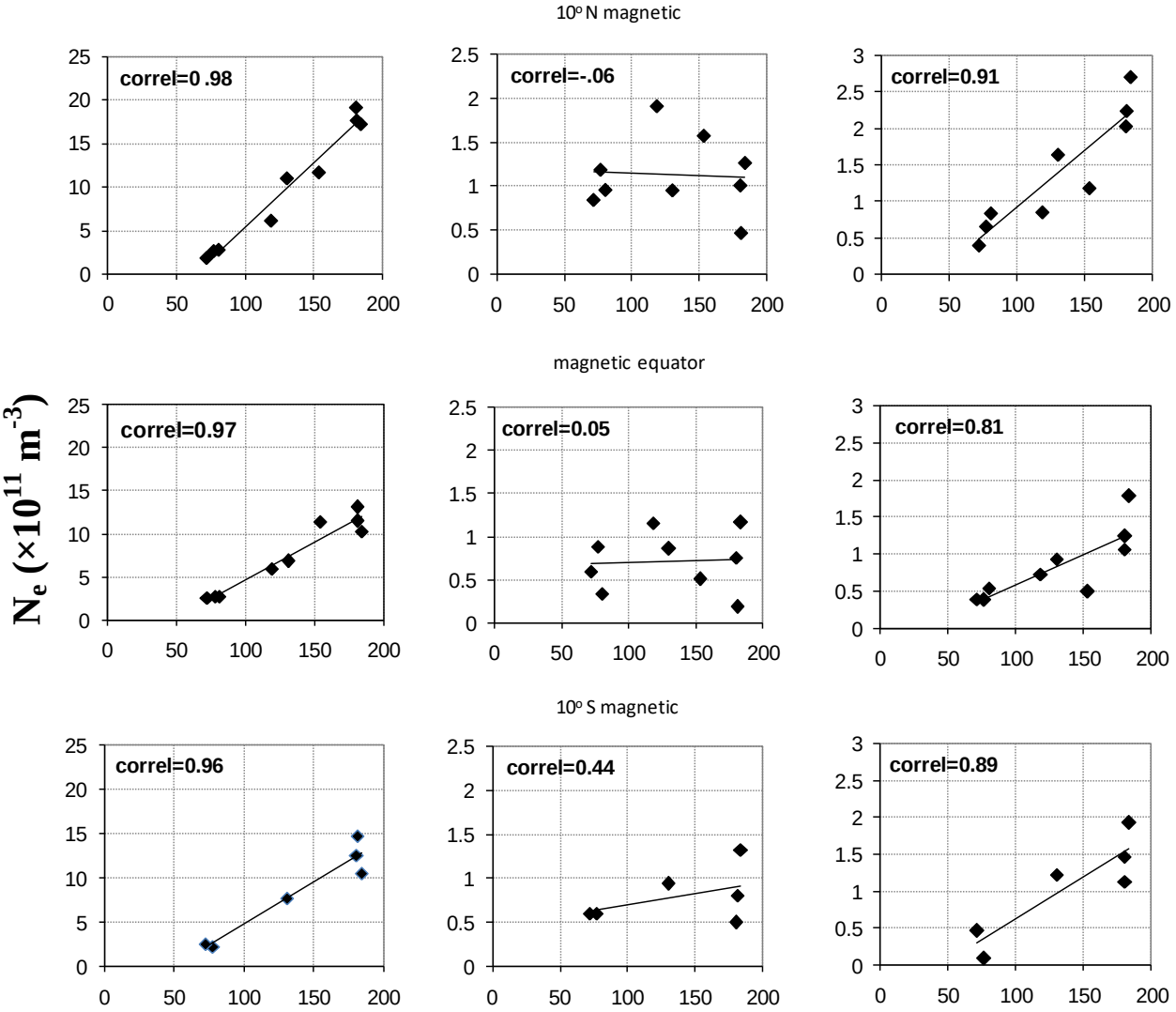

F10.7 flux

Amplitude of mean, annual and semiannual components of Ne (from left to right) plotted against 10.7 cm solar flux at three latitudes for day time (10:00-14:00 LT).

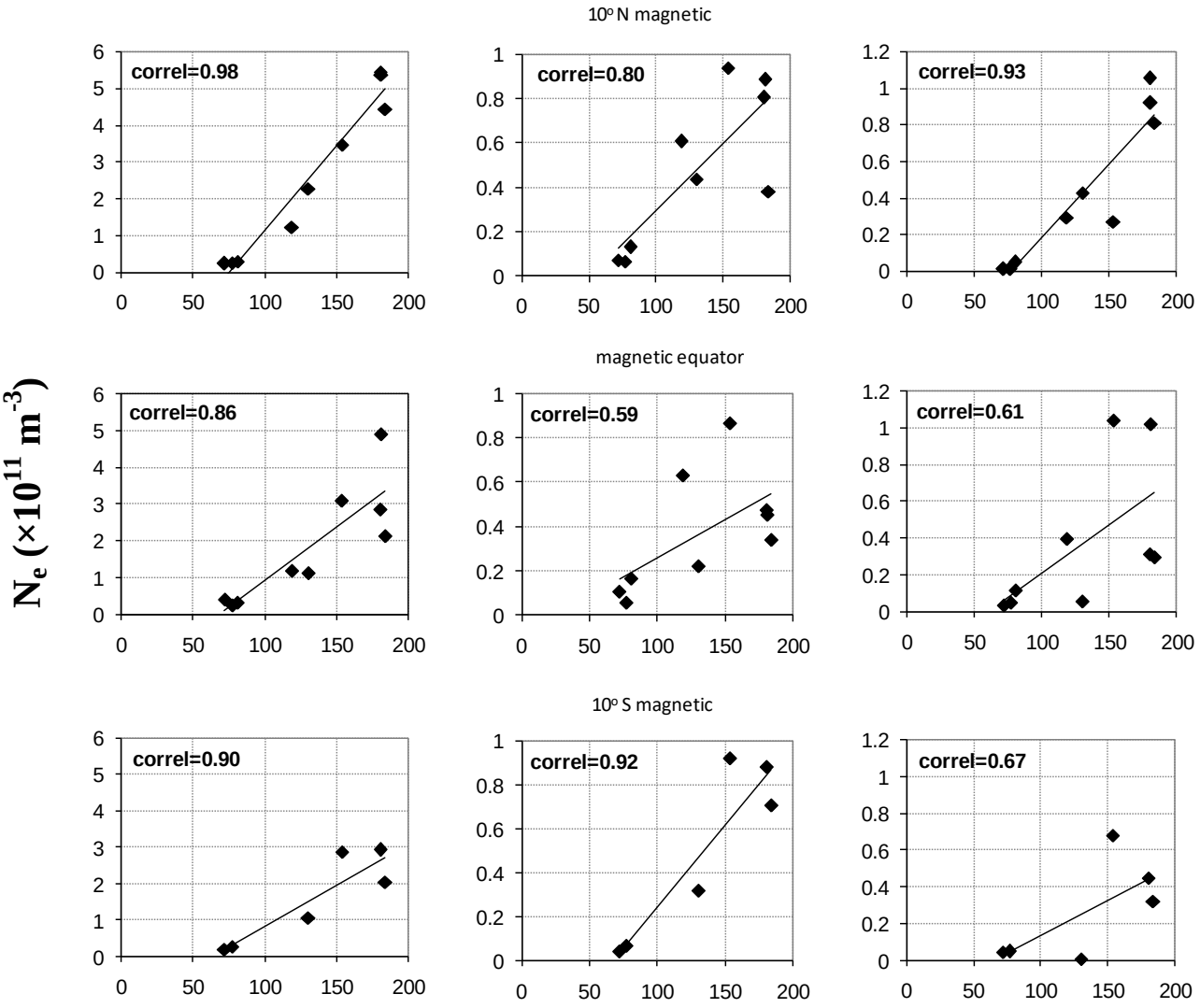

F10.7 flux

Amplitude of mean, annual and semiannual components of Ne (from left to right) plotted against 10.7 cm solar flux at three latitudes for night time (22:00-00:00 LT).

Table III: Annual mean, annual and semiannual amplitude and phases over 10^{o} N magnetic

	Year	Annual mean (a_o) ($x10^{11}$ m^{-3})	Amplitude		Phases	
			a_1 ($x10^{11}$ m^{-3})	a_2 ($x10^{11}$ m^{-3})	Φ_1 (radians)	Φ_2 (radians)
DAY	1995	2.56	1.19	0.66	5.21	4.11
	1996	1.77	0.85	0.41	4.76	3.35
	1997	2.71	0.96	0.84	4.63	3.3
	1998	6.07	1.91	0.86	4	2.82
	1999	11.63	1.57	1.19	3.83	2.89
	2000	17.62	0.48	2.24	3.11	3.22
	2001	17.19	1.27	2.70	0.70	3.05
	2002	19.11	1.01	2.03	5.57	4.34
	2003	10.95	0.96	1.64	5.59	3.5
NIGHT	1995	0.26	0.07	0.01	2.94	4.71
	1996	0.24	0.07	0.01	3.23	0.16
	1997	0.28	0.13	0.05	1.46	2.74
	1998	1.22	0.61	0.29	1.8	3.41
	1999	3.48	0.94	0.27	1.28	1.74
	2000	5.37	0.89	0.92	4.79	3.57
	2001	4.43	0.38	0.81	3.03	3.40
	2002	5.45	0.81	1.05	4.39	3.72
	2003	2.27	0.44	0.43	4.54	3.33

Table IV: Annual mean, annual and semiannual amplitude and phases over 0^o magnetic

	Year	Annual mean (a_o) ($x10^{11}$ m^{-3})	Amplitude		Phases	
			a_1 ($x10^{11}$ m^{-3})	a_2 ($x10^{11}$ m^{-3})	Φ_1 (radians)	Φ_2 (radians)
DAY	1995	2.76	0.81	0.38	5.52	4.08
	1996	2.50	0.59	0.38	4.86	3.70
	1997	2.70	0.34	0.54	4.69	3.45
	1998	5.90	1.16	0.73	3.26	2.92
	1999	11.36	0.50	0.49	2.89	2.68
	2000	13.11	0.18	1.24	5.85	3.00
	2001	10.27	1.17	1.78	0.66	2.68
	2002	11.50	0.76	1.06	6.22	4.13
	2003	6.79	0.86	0.93	5.32	3.88
NIGHT	1995	0.24	0.05	0.05	1.4	3.49
	1996	0.40	0.10	0.03	4.69	3.75
	1997	0.32	0.16	0.11	0.89	2.14
	1998	1.18	0.63	0.39	1.22	2.68
	1999	3.09	0.87	1.04	0.78	2.66
	2000	4.90	0.45	1.02	6.15	3.48
	2001	2.13	0.34	0.29	0.52	2.87
	2002	2.86	0.47	0.31	5.51	4.12
	2003	1.12	0.22	0.05	5.30	3.37

Table V: Annual mean, annual and semiannual amplitude and phases over 10^{o} S magnetic

	Year	Annual mean (a_o) ($x10^{11}$ m^{-3})	Amplitude		Phases	
			a_1 ($x10^{11}$ m^{-3})	a_2 ($x10^{11}$ m^{-3})	Φ_1 (radians)	Φ_2 (radians)
DAY	1995	2.19	0.60	0.09	5.74	4.51
	1996	2.49	0.60	0.46	5.24	3.45
	1997					
	1998					
	1999					
	2000	14.65	0.80	1.12	4.54	3.49
	2001	10.47	1.31	1.92	0.73	2.78
	2002	12.53	0.50	1.46	5.87	4.08
	2003	7.60	0.94	1.21	5.75	3.68
NIGHT	1995	0.26	0.06	0.05	1.25	3.48
	1996	0.19	0.04	0.04	0.90	1.64
	1997					
	1998					
	1999	2.87	0.92	0.68	0.89	2.76
	2000					
	2001	2.04	0.70	0.32	0.64	2.68
	2002	2.93	0.88	0.45	5.93	4.19
	2003	1.05	0.32	0.01	6.18	5.67

mean values of F10.7: 77, 72, 81, 119, 153, 181, 184, 180, 130 for the years 1995, 1996, 1997, 1998,1999, 2000, 2001, 2002 and 2003 respectively. Table VI shows the percentage increase of O/N_2 ratio at noon in spring and autumn over that in summer as derived from the MSIS-2000 model. The O/N_2 ratio in spring is higher than the autumn over 10^o S magnetic and over 10^o N magnetic, where autumnal O/N_2 ratio is slightly higher than the vernal O/N_2 ratio irrespective of solar activity.

Table VII shows the percentage increase of O/N_2 ratio in equinoxes above the value in summer at midnight (0:00 LT) over ± 10^o magnetic and over the magnetic equator derived from MSIS-2000 model. The model is in agreement with observations over 10^o S magnetic and over magnetic equator for moderate and high solar activity and over 10^o N magnetic for low solar activity.

2.4 CAUSES OF ANNUAL AND SEMIANNUAL VARIATION

The annual and semiannual variations in electron density of the F region have been considered to be due to one or more of the following mechanisms:

1. Composition changes due to global thermospheric circulation – the mechanism studied by Millward et al. (1996) and Rishbeth et al. (2000).
2. Variations in geomagnetic activity.
3. Solar wind energy (Lal. 1992, 1998).
4. Inputs from below, due to atmospheric waves and tides.
5. Changes in atmospheric turbulence.
6. Anisotropy of solar EUV emission in solar latitude (Burkard, 1951).

As suggested by Fuller-Rowell (1998) the semiannual anomaly is caused by the "thermospheric spoon", i.e., the global thermospheric circulation at solstices raises the molecular nitrogen and oxygen densities and therefore reduces the atomic oxygen density compared with the equinoxes. Because N_2 and O control the loss rate and production rate of the plasma respectively, a low O/N_2 ratio gives rise to low electron densities in the ionosphere. The O/N_2 ratio depends on motions and chemical changes driven by solar radiation absorbed within the thermosphere.

No one to one correlation has been found between the electron density and geomagnetic activity over the Indian zone. The MSIS-2000 model simulations produce a

Table VI: Percentage of increase of O/N2 ratio derived from MSIS-2000 model at noon in the equinoxes over those in summer

Year	10^o S magnetic		0^o magnetic		10^o N magnetic	
	spring	autumn	spring	autumn	spring	autumn
1995	-3	-7	2	0.3	7	9
1996	-4	-8	1	-1	6	7
1997	-2	-7	3	1	8	10
1998	3	-2	10	8	17	18
1999	5	1	13	11	20	22
2000	7	2	15	13	23	25
2001	7	2	15	13	23	25
2002	7	2	15	13	23	24
2003	4	-1	11	9	18	20

Table VII: Percentage of increase of O/N2 ratio derived from MSIS-2000 model at night (00:00 hr.) in the equinoxes over those in summer

Year	10^o S magnetic		0^o magnetic		10^o N magnetic	
	spring	autumn	spring	autumn	spring	autumn
1995	-3	-7	2	0.3	7	9
1996	-4	-8	1	-1	5	7
1997	-2	-7	3	1	20	22
1998	3	-2	10	8	16	18
1999	5	0.5	13	11	20	22
2000	7	2	15	13	23	25
2001	7	2	15	13	23	25
2002	7	2	15	13	23	24
2003	4	-1	11	9	18	20

reasonably good representation of the annual and semiannual variations of Ne for low geomagnetic activity condition.

Lal (1992, 1998) regards the “solar wind” as the cause of all semiannual aeronomic phenomena. The solar wind is on the other hand connected to the geomagnetic activity. For example, according to the theory of Russell and McPherron (1973), the semiannual variation of geomagnetic activity depends on the varying geometrical coupling of the interplanetary and terrestrial magnetic fields.

Zou et al. (2000) have studied about how waves and tides in the underlying mesosphere may affect the F2 layer, but they concluded that they are unlikely to have a major effect on annual and semiannual variations of NmF2.

Regarding the mechanism of changes in atmospheric turbulence, Shimazaki (1972) showed that large-scale convection motions have much more effect on thermospheric composition than changes in eddy diffusion at the turbopause, even though the “spoon” terminology might be thought to imply increased turbulent mixing.

The hypothesis that the Sun’s EUV radiation varies with heliographic latitude (Burkard, 1951), combined with the semiannual variation of the Earth’s heliographic latitude, is dismissed due to lack of evidence to support it.

2.5 CONCLUSION

The annual and semiannual variation of ionospheric parameters in the equatorial F-region has been studied in various regions of the world and its existence has been proved by experimental evidences. Yearly variations of the F-region electron density in the Indian zone have been investigated using SROSS C2 and FORMOSAT – 1 data. The observations show the existence of an equinoctial asymmetry over India with higher values of electron density in spring than in autumn during daytime. At night electron density in autumn becomes higher than in spring for low solar activity while for moderate and high solar activity Ne in spring is

higher than that in autumn. Daytime annual and semiannual variation has no latitudinal variation while nighttime annual and semiannual variation shows latitudinal variation. We find that annual and semiannual variation has well-defined relationship with solar activity. The semiannual variation has almost constant phase near equinox and its amplitude increases with increasing F10.7 both during daytime and nighttime over all the three latitudes. Daytime annual variation is unaffected by solar activity with very poor correlation of its amplitude with F10.7. But at night the amplitude of the annual variation of electron density increases with increasing F10.7.

ACKNOLEDEGEMENT

Authors wish to express their sincere thanks to National Space Organization (NSPO), for the FORMOSAT-1 data.

REFERENCES

1. Moffet R. J., The equatorial anomaly in the electron distribution of the terrestrial F-region. Fundamental Cosmic Physics. 1979; 4, 313 – 391.
2. Anderson D. N., Modelling the ambient, low latitude F-region ionosphere- a review. J. Atmos. Terr. Phys. 1981; 43, 753 – 762.
3. Walker G. O., Ma T. H. K., Golton E., The equatorial ionosphere anomaly in electron content from solar minimum to solar maximum for South East Asia. Ann. Geophys. 1994; 12, 195.
4. Baily G. J. and Balan N., A low latitude ionosphere plasmasphere model. STEP handbook of ionospheric models. In: Schunk R. W. (Ed), STEP Handbook of Ionospheric Models. Scientific Commission on Solar Terrestrial Physics and Utah State University, USA. 1996; 173 – 206.
5. Rishbeth H., The theoretical F-layer: progress and puzzles. Ann. Geophys. 2000; 18, 730 – 739.
6. Bhuyan P. K., Chamua M., Subrahmanyam P., Garg S. C., Diurnal, seasonal and latitudinal variation of electron temperature measured by the SROSS C2 satellite at ~500 km altitude and comparison with the IRI. Ann. Geophys. 2002a; 20, 807 – 815.
7. Bhuyan P. K., Kakakoty P. K., Garg S. C., Subrahmanyam P., Electron and ion temperature and electron density at $+10^{o}$ magnetic latitude from SROSS C2 measurements over India and comparison with the IRI. Adv. Space Res. 2002b; 29(6), 865 – 870.
8. Niranjan K., Sridhar H. S., Rama Rao P. V. S., Garg S. C., Subrahmanyam P. Evening enhancements in F – region electron temperature at subtropical latitudes during Summer in the Indian SROSS C2 RPA data. J. Atmos. Solar Terr. Phys. 2003; 65, 813 – 819.

9. Bhuyan P. K., Chamua M., Subrahmanyam P., Garg S. C., Effect of solar activity on diurnal and seasonal variations of electron temperature measured by the SROSS C2 over Indian low latitudes. Adv. Space Res. 2006; 37, 885 – 891.
10. Rishbeth H., and Muller-Wodarg I. C. F., Vertical circulation and thermospheric composition: a modelling study. Ann. Geophysicae. 1999; 17: 794-805.
11. Zou I., Rishbeth H., Muller-Wodarg I. C. F., Aylward A. D., Millward G. H., Fuller-Rowell T. J., Idenden D. W., Muffett R. J., Annual and semi-annual variations in the ionospheric F2-layaer. I. Modelling. Ann. Geophysicae. 2000; 18, 927-944.
12. Zhao B., Wan W., Liu L., Mao T., Ren Z., Wang M., Features of annual and semi-annual variations derived from the global ionospheric maps of total electron content. Ann. Geophysicae. 2008; 25, 2513 – 2527
13. Yufei He, Dongmei Yang, Rong Zhu, Jiadong Qian and M Parrot, Variations of electron density and temperature in ionosphere based on the DEMETER ISL data. Earthq. Sci. 2010; 23, 349 – 355.
14. Zheng W., Jiankui S., Guojun W., Xiao W., Zherebtov G. A., Romanova E. B., Ratovsky K.G., Polekh N. M., Diurnal, seasonal, annual, and semi-annual variations of ionospheric parameters at different latitudes in East Asian sector during ascending phase of solar activity. Solar-Terrestrial Physics. 2016; 3, 43 – 50.
15. Garg S. C. and Das U. N., Aeronomy experiment on SROSS C2. J. Spacecraft Technology. 1995; 5, 11 – 15.
16. Nurtaev B., Observation and measurement of solar activity for study of climate trends. International Journal of Science and Engineering Investigations. 2018; 7(81), 2251 – 8843.
17. Su Y. Z., Bailey G. J., Oyama K. I., Annual and seasonal variations in the low-latitude topside ionosphere. Ann. Geophysicae.1998; 16, 974-985.
18. Picone J. M., Hedin A. E., Drob D. P., Aikin A. C., NRLMSISE-00 empirical model of the atmosphere: statistical comparison and scientific issues. J. Geophys. Res..2002; 107(A12), 1468.

19. Millward G. H., Rishbeth H., Moffett R. J, Quegan S., Fuller-Rowell T. J., Ionospheric F2 layer seasonal and semi-annual variations. J. Geophys. Res..1996; 101, 5149-5156.
20. Rishbeth H., Muller-Wodarg I. C. F., Zou L., Fuller-Rowell T. J., Millward G. H., Moffett R. J., Idenden D. W., Aylward A. D., Annual and semi-annual variations in the ionospheric F2-layer: II. Physical discussion. Ann. Geophysicae. 2000; 18, 945-946.
21. Lal, Chaman, Global F2 layer ionization and geomagnetic activity. J. Geophys. Res..1992; 97, 12 153-12 159.
22. Lal, Chaman, Solar wind and equinoctial maxima in geophysical phenomena. J. Atmos. Terr. Phys. 1998; 60, 1017-1024.
23. Burkard O., Die halbjahrige Periode der F2-Schicht-Ionisation. Archiv. Meteoral. Biokim. Wien. 1951; 4, 391-402.
24. Fuller-Rowell T. J., The thermospheric spoon" a mechanism for the semi-annual density variation. J. Geophys. Res. 1998; 103, 3951-3956.
25. Russel C. T., McPherron R. L., Semi-annual variation of geomagnetic activity. J. Geophys. Res. 1973; 78, 92-107.
26. Shimazaki T., Effects of vertical mass motions on the composition structure in the thermosphere. Space Research. 1972; 12, 1039-1045.

FIGURE CAPTIONS

Fig. 1 Yearly variation of electron density during daytime at 500 km altitude.

Fig. 2 Yearly variation of electron density during nighttime at 500 km altitude.

Fig. 3 Periodogram of electron density during daytime over 10^{o} N magnetic.

Fig. 4 Periodogram of electron density during daytime over 0^{o} magnetic.

Fig. 5 Periodogram of electron density during daytime over 10^{o} S magnetic.

Fig. 6 Periodogram of electron density during nighttime over 10^{o} N magnetic.

Fig. 7 Periodogram of electron density during nighttime over 0^{o} magnetic.

Fig. 8 Periodogram of electron density during nighttime over 10^{o} S magnetic.

Fig. 9 Amplitude of mean, annual and semiannual components of Ne (from left to right) plotted against 10.7 cm solar flux at three latitudes for day time (10:00-14:00 LT).

Fig. 10 Amplitude of mean, annual and semiannual components of Ne (from left to right) plotted against 10.7 cm solar flux at three latitudes for night time (22:00-00:00 LT).